A PULSE ANALYSIS SYSTEM AND COMPUTER PROGRAM FOR THE ROSSI LET COUNTER*

ROBERT F. DVORAK
Argonne National Laboratory, Argonne, Illinois, U.S.A.

Abstract—Acceptance of the Rossi LET counter for routine health physics use depends upon the degree to which data collection and analysis can be simplified. This paper describes an electronic system for recording counter events and a computer program prepared for data analysis that contribute toward this end.

In developing this system, we found that spectral stability is significantly affected by voltage and gas purity through the mechanism of varying ion collection time. Circuitry has been developed which delays sampling of the pulse height until full charge collection has been achieved. Operation as a sealed chamber has thereby been achieved over useful periods.

Since the spectra realized are typically exponential in shape, extremely long data collection times are required to achieve statistical significance for the large pulses. To ameliorate this problem, an analog pulse height computer is used to compress the high energy deposition end of the spectrum according to a selectable power function before pulse height analysis is performed.

The data analysis program has been made as flexible as possible to allow further studies in interpretive procedure. The raw data for both radiation field and background (where applicable) are smoothed before determining net counts. The technique used has a minimum of bias as to the spectrum shape. The smoothed spectrum is then analyzed and a probable LET spectrum determined. Since the energy loss spectrum due to mono-LET particles traversing the chamber depends on questionable assumptions, options are included for triangular, exponential, and square stripping functions. From the LET spectrum, the dose and dose equivalent are calculated, and the LET spectrum is smoothed and plotted. Examples are given of the results produced by the system for typical radiation sources.

INTRODUCTION

An instrument capable of measuring the dose equivalent in a radiation field where nothing is known or assumed about the nature of the field would be an extremely valuable tool to the biologist, biophysicist, and health physicist. If this tool is to be useful, it must meet some reasonable requirements involving simplicity and reliability. The Rossi LET chamber,[1] with associated gas supply system, electronics, and calculation techniques as employed today are too complex for routine use in applied Health Physics. This paper describes the work we have done at Argonne National Laboratory to simplify the necessary systems to a point where the Rossi LET chamber can be used reliably and with greater convenience by a health physicist. Utilization of the detector and supporting components must still be restricted to situations where the need for information is sufficiently important as to warrant the cost and time incidental to the use of this instrument.

LET CHAMBER

The Rossi LET chamber is a proportional counter in spherical geometry having a tissue equivalent wall and utilizing a tissue equivalent fill gas. Figure 1 is an X-ray photograph of the 8-in. diameter counter fabricated for us by Dr. H. H. Rossi. In the photograph, the 0.25 in. thick wall of muscle equivalent conductive plastic[2] is seen enclosing a 4100 cc chamber

* Work performed under the auspices of the United States Atomic Energy Commission.

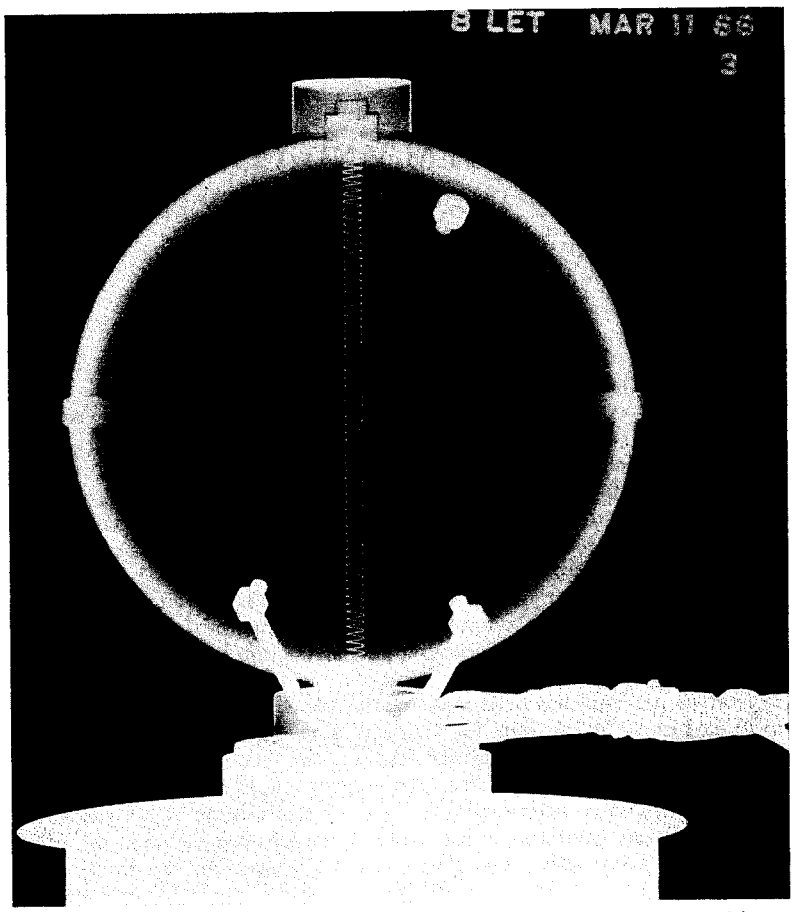

FIG. 1. X-ray photograph of 8-in. diameter LET counter. The opaque object at the upper right is a source holder, objects near bottom are gas inlet and outlet.

cavity. A rather complex sub-assembly penetrating the top and bottom of the sphere supports the 0.25 in. thick diameter grid coil of 0.010 in. diameter stainless steel wire, and accurately locates and supports a concentric 0.0005 in. diameter anode of the same material.

In use, the outer wall is at ground potential, the anode is at a pressure dependent positive potential, and the grid coil is fixed at 50% of the anode potential by a resistive divider. The following sequence of actions occurs in the two regions of the counter. Electrons liberated in the cavity by an ionizing event drift toward the grid under the influence of the electric field. In the region of the grid, the electrons are accelerated toward the anode by the anode field. Proportional multiplication is achieved in a small volume surrounding the anode. The grid serves the dual function of (1) gathering electrons and negative ions and (2) accurately defining the potential gradient in the proportional region of the counter.

The physical analogy simulated by this chamber when it is placed in a radiation field is not entirely clear, but for considerations of radiation equilibrium, the event spectrum should be similar to that at the geometric center of a tissue slab 0.5 in. thick and 8.5 in. in diameter. In setting up the mathematical expressions for the probable cavity path distributions, one must remain with the physical reality (for the chamber described) of a spherical 8 in. diameter cavity that is filled with tissue equivalent gas at low pressure, and is surrounded

by a 0.25 in. thick tissue equivalent wall of approximately tissue density.

Since calibration of energy loss is not direct, but rather is achieved by projecting a collimated beam of alpha particles across a chamber diameter, one is forced to accept the calibration constant

$$K = \frac{\text{LET}_\infty \times \text{chamber diameter}}{\text{pulse height}}$$

as determined with alpha particles to be the same for protons, mesons, electrons, etc. As has been indicated elsewhere,[3] there are a number of additional complications at low particle energies and small effective cavity diameters that can lead to errors in the spectrum, dose, and dose equivalent calculations. However, these errors are probably minor in view of the uncertainties in the LET effect of radiation on biological systems at and below the diameter of a single cell, and the relationship between sub-cellular damage and over-all radiation effect to systems containing a large number of cells.

If one can accept these limitations to accuracy, it is possible to calculate a dose and dose equivalent for the radiation field at the chamber location for the tissue geometry simulated by the chamber.

GAS HANDLING SYSTEM

The Rossi LET chamber is generally used in a continuous gas flow mode to minimize the effects of possible minor leaks, preferential diffusion of fill gas constituents into the plastic wall, and outgassing of detrimental gases and vapors from the wall. The gas system used by Rossi has been illustrated in the literature.[4]

It was decided at the beginning of this development project that the proportional counter would have to be liberated from the gas flow system if any reasonable flexibility of use was to be achieved. When the chamber is used in a periodic-fill mode, the gas handling system is greatly simplified. A schematic of our system is shown in Fig. 2. The transducer for pressure measurement is a simple ionization chamber having the cathode coated with about 500 μc of promethium-147, a fairly low energy beta emitter. Current from the chamber anode is measured by a vibrating reed electrometer. The transducer must be calibrated for the specific fill gas against appropriate mechanical gauges. This method of pressure measurement has no particular advantage over the use of mechanical gauges except in range of measurement, which is from atmospheric down to approximately 0.1 mm. A photograph of the cart-mounted fill station is shown in Fig. 3.

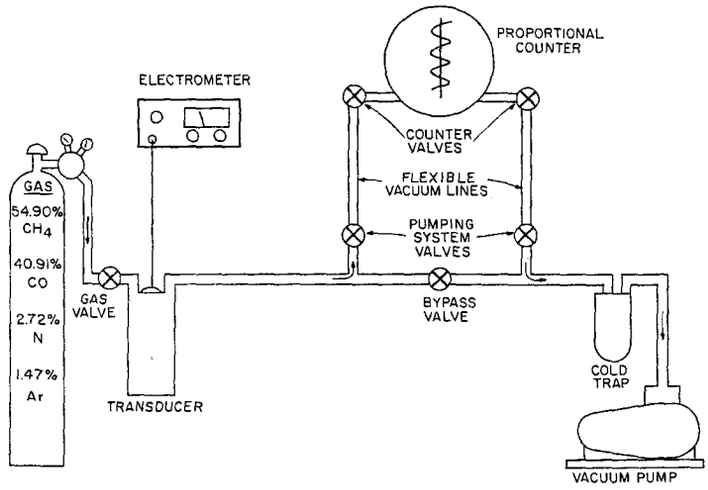

FIG. 2. Schematic of gas handling system for periodic-fill operation.

The fill gas used at present has a composition:

54.90% methane
40.91% carbon monoxide
2.72% nitrogen
1.47% argon

This mixture has an advantage over the more common methane–carbon dioxide–nitrogen mixture[5] in that all components have very similar coefficients of diffusion into the Shonka plastic. It is less than half as expensive as the ethane, ethylene, nitrogen, and neon mixture used by Kastner, Rose, and Shonka,[6] and retains a significant number of oxygen atoms.

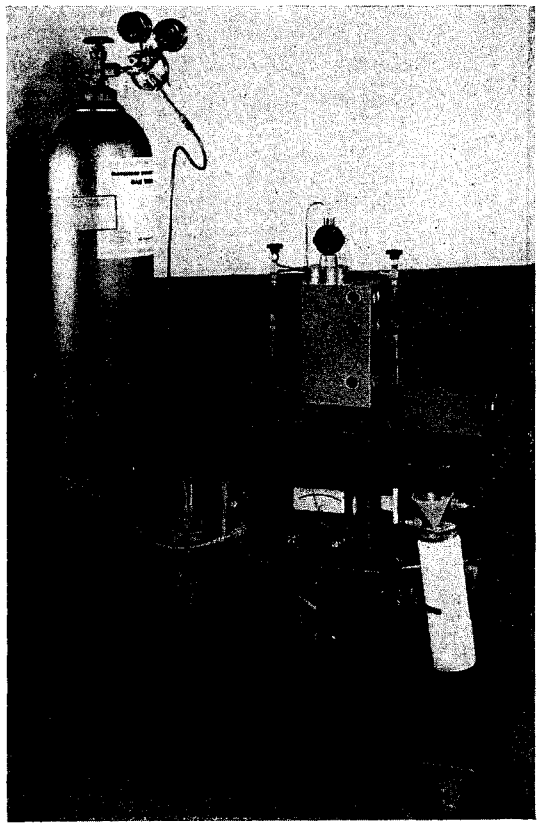

FIG. 3. Cart-mounted gas handling system, showing 2-in. LET chamber and preamplifier in filling position.

When this gas was used under periodic fill conditions, it was found that the multiplication is not completely stable with time, even with extended outgassing prior to filling. The multiplication for the first 8 hr after filling proved to be essentially stable, as shown in Fig. 4. However, an initial aging period of at least 10 min is required during which the multiplication shows a decrease of 1–2%. After 72 hr, the multiplication decreases an additional 6% with no apparent resolution loss. Changes in ambient temperatures appear to be more troublesome, although no quantitative evaluation has yet been achieved.

Under reasonable thermal conditions, the change in proportionality (and hence the calibration constant) is less than 1% in 8 hr. We feel that this does not lead to excessive data error. The data shown here were taken with the 8-in. diameter chamber. With the 2-in. chamber, stability appears to be better.

ELECTRONIC SYSTEM

Several mechanisms have been found which affect the detector pulse shape. First, the time required for full ion collection becomes steadily greater as the gas ages, beginning at 1 or 2 μsec for fresh gas, and eventually exceeding 20 μsec. Second, this collection time is a function of the collection (grid) voltage. Third, at any particular time there will be variations as great as a factor of two in ion collection time, probably depending on location of the ionizing particle track segment within the chamber. Under the described conditions, it is clear that differentiation of the signal pulse cannot be tolerated, and sampling of the pulse height must be delayed until full charge collection is achieved if maximum system stability is to be attained.

This electronic system is designed to take these restrictions into account, and is shown schematically in Fig. 5. The voltage sensitive preamplifier, which serves as a mechanical base for the detector, is a highly modified Oak Ridge design featuring a very low input noise level and very long time constants throughout. The response of the preamplifier to a step function input signal is an output pulse with a rise-time of 80 nsec, and a decay time of 6.8 msec. The gain is 25. In our application, the voltage pulse from the preamplifier is the integral of the charge collected on the input capacitance.

Since, at useful pulse repetition rates, long duration pulses such as these would cause

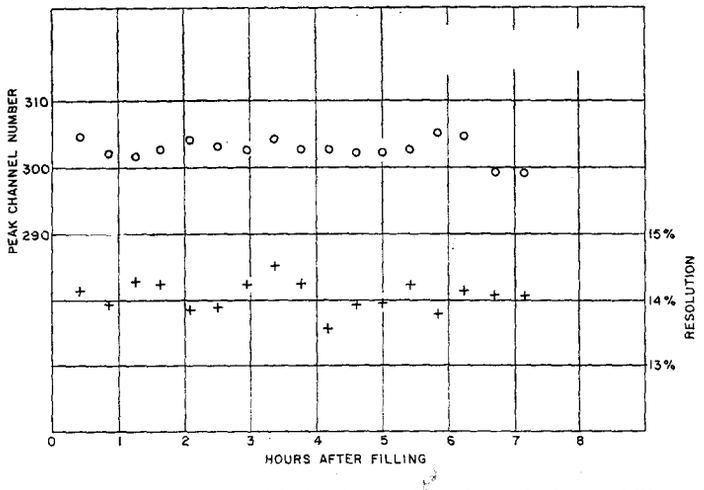

FIG. 4. Determination of chamber multiplication and peak resolution stability. A collimated beam of curium-244 alpha particles projected across a chamber diameter was the source of pulses. The fill pressure was 9 mm.

disturbing bias shifts through pulse pileup, the next circuit element is the Argonne PA 95-B delay line clipper. The pulse may be terminated by reflection at 4, 8, 12, or 16 μsecs, the choice being determined by the conditions under which the measurement is to be made.

Final pulse amplification is performed by the Argonne LPA-5 amplifier. The over-all system response to a step function input signal is an amplifier output pulse with a rise-time of 0.45 μsec and a decay time of 800 μsec that is terminated by the clipper reflection after the selected delay interval. The overall gain of the preamplifier, clipper, and linear amplifier is 1460.

A serious problem with a detector of this type is that the typical pulse height spectrum is roughly exponential in shape. The number of small pulses taxes the memory capacity of the multichannel pulse height analyzer during the time that the number of large pulses per analyzer channel is still statistically very low. It is our feeling that improved statistical accuracy in the number of these high energy loss events is more important than precision in the energy loss determination for each event.

An analog pulse height computer is now

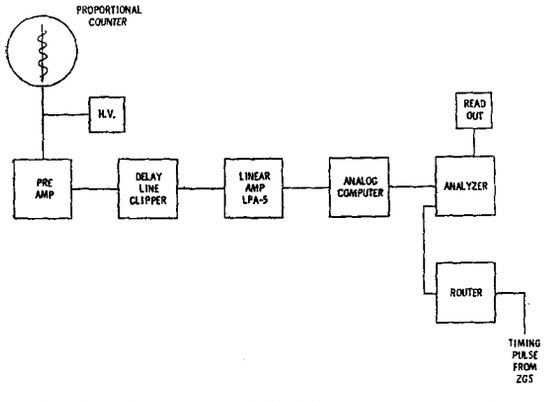

FIG. 5. Schematic of LET system electronic components.

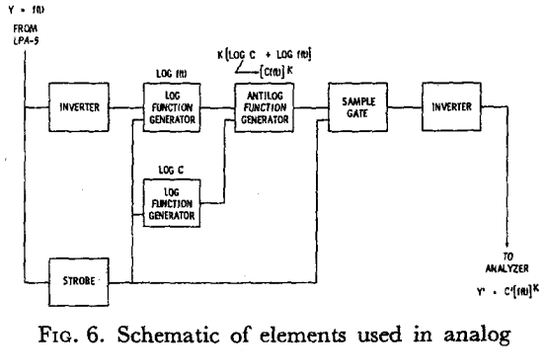

FIG. 6. Schematic of elements used in analog pulse height computer.

available[7] which can perform a spectrum compression that materially aids in this data collection problem. The combination of elements that has been most useful to us is shown schematically in Fig. 6. In our application, the output pulse of the LPA-5 amplifier is analyzed, and a computer output pulse is generated having an amplitude that is a power function of the input pulse height. The pulse shape is square, about 1.5 μsec long, and between zero and + 10 V in height, compatible to almost any pulse height analyzer.

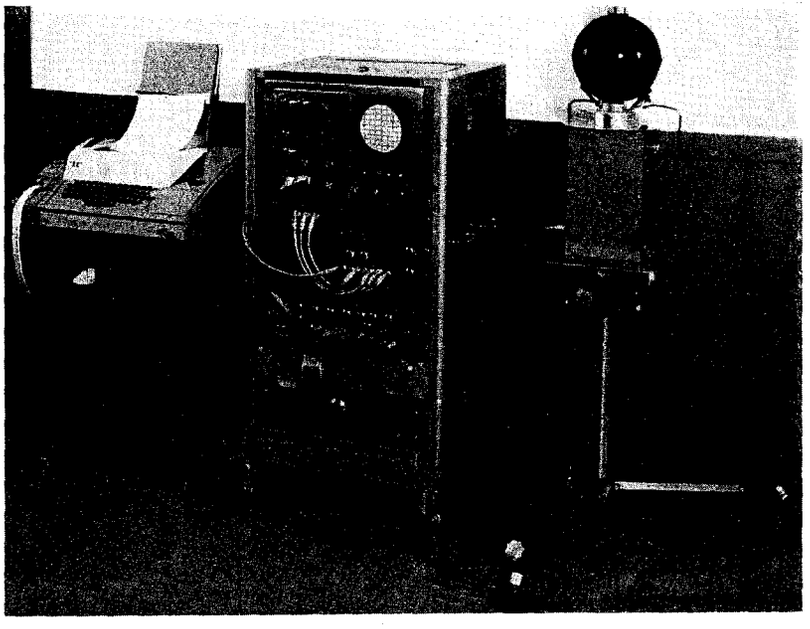

FIG. 7. Component of LET system as used in field measurements. Rack cabinet contains, from top to bottom, the 400 channel pulse height analyzer, the ETC chassis containing amplifier, clipper, router and preamplifier power supply, the analog computer, a high voltage power supply, and a test pulse generator.

The exponent function normally used, 0.5, is near the computer's lower limit of 0.4, and is chosen for simplicity in system calibration. For any exponent less than one, the desired expansion of energy scale for low energy loss pulses and compression of high energy loss pulses is achieved.

The pulses are fed to a 400 channel Victoreen PIP analyzer which has a memory capacity of 10^6 events per channel. In measurements of continuous emission radiation sources, we generally use one quadrant (100 channels) of the memory, and hence can store a total of four separate runs before readout must be made. For measurements of pulsed sources, as at the Argonne Zero Gradient Synchrotron, a routing circuit controls the analyzer. This circuit is triggered by a pulse from the accelerator at the approximate time of proton injection into the ring. The analyzer is gated on and pulses are routed to the first memory quadrant for a preselected interval of time sufficient to cover the entire machine spill period. The analyzer then is held off for a second preselected interval during which routing is changed to the third memory quadrant. Background then is counted for the same length of time as was selected for the machine spill period. The analyzer finally is gated off until the next accelerator timing pulse. In this fashion, the contribution by background events is minimized in the "machine on" memory quadrant and an additional run with accelerator off is not required for background determination. A second pair of runs

can be made in quadrants two and four before readout is required.

The data is delivered in two forms. The total events per channel are simultaneously recorded by tabulated typewriter printout and punched paper tape in ASCII format. The paper tape is then used to prepare the data deck of IBM cards in a format compatible to the computer program. A photograph of the entire system is shown in Fig. 7.

COMPUTER PROGRAM

The most tedious and time-consuming aspect of LET counter utilization is the data analysis. To make application of the counter more attractive to health physics personnel, a computer program was included as part of the instrument development program. A successful program, which requires less than one minute of CDC 3600 computer time has been prepared. In practice, full processed results are available in about 2 hr. The program consists of six steps, of which a number are superfluous to the end point but necessary for careful evaluation of the data.

1. Input data constants are printed out providing run identification, analog computer power function, a channel calibration constant relating channel number to energy loss for the event, keV to ergs conversion constant, fill gas weight, diameter of chamber cavity in terms of equivalent tissue thickness, the exponent for exponential stripping option, the time over which the source data was taken, and the time over which the background data was taken.

2. The raw input data is smoothed using the following technique: To smooth the point K we must consider the sequence of points from $K-2$ to $K+3$. We postulate first that data shall be conserved and that any correction made to K will be compensated in the adjacent channels $K-1$ and $K+1$. We also postulate that no correction will be made unless the necessary compensating correction to K − 1 brings it closer to the average of $K-2$, $K-1$, and K and the correction to $K+1$ bring it closer to average of K, $K+1$, and $K+2$.

The magnitude of the correction is determined by fitting to a cubic curve through construction of a difference table, as indicated in Fig. 8. Setting the fourth differences, $\nabla_4(K)$ and $\nabla_4(K+1)$ equal to zero, one can solve for both β and Δ and the best correction to a cubic curve can be calculated. In the computer program, corrections of only $\frac{\Delta}{20}$ and $\frac{\beta\Delta}{20}$ are applied successively to each K in the spectrum. This smoothing cycle is repeated 100 times.

The raw and smoothed values of both the source and background spectra, as well as the difference between smoothed source and smoothed background spectra are printed out in parallel column format for inspection.

3. The effect of the smoothing program is examined in a rather crude fashion to determine

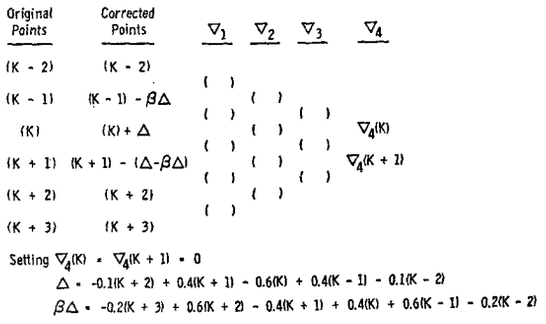

FIG. 8. Conceptual schematic of technique for smoothing a point K. The difference table is indicated and the equations for magnitude of and distribution of the correction are explicitly stated.

where the smoothing has altered a point outside a normal statistical error from the initial data. The first column is the channel number; second column, the square root of the raw event count; third column, the difference between the raw event counts and the smoothed counts; fourth and fifth columns, the same as the second and third except applied to the background counts. In the sixth column, the symbol (1) appears where the difference between smoothed and raw counts exceeds in magnitude the square root of the raw counts for either events or background, and the symbol (2) where the difference is greater than twice the square root of the raw counts.

4. The smoothed data points are normalized

to the proper unit time and analyzed by a subroutine in which the energy loss by events in each energy loss interval is computed and summed. The printout consists of interval number, source counts per unit time, background counts per unit time, energy in keV at the upper limit of the interval, energy in keV at the center of the interval, deposited dose rate for the interval, and cumulative dose rate. The deposited dose rate for the run is the value of cumulative dose rate for the highest K interval.

5. The distribution of events in LET is now determined and from this the dose and dose equivalent distributions in LET are calculated.

Before a calculation can be started, a decision must be made as to the most probable distribution in path lengths for an ionizing particle traversing the chamber. In general, one has no knowledge as to where (in the gas, wall, or exterior environment) a particular event originated and what its actual path length was in the chamber. Rossi and Rosenzweig,[1] and more recently Caswell,[8] have presented arguments leading to a triangular distribution in path lengths for events originating in the cavity wall and traversing the chamber, where the probability per unit path length is directly proportional to the path length. My own feeling is that the assumption of a square spectrum (all path lengths equally probable) also is logically supportable, and that particular cases ranging from square through exponential distributions of the form $A(1 - e^{-\mu})$ to triangular can be demonstrated. In addition, a superimposed

M_{ij} = Number of Events in LET Interval j Which Traverse the Chamber with an Energy Loss in the Interval i

$$M_{ij} = \Delta_i\left[\frac{N_j}{\Delta_j} - \frac{N_{j+1}}{\Delta_{j+1}}\right]$$

For Square Path Distribution $\Delta_\ell = E_\ell - E_{\ell-1}$

Triangular Path Distribution $\Delta_\ell = E_\ell^2 - E_{\ell-1}^2$

Exponential Path Distribution $\Delta_\ell = \left[(E_\ell - E_{\ell-1}) - \frac{1}{\beta}\left(e^{-\beta E_{i-1}} - e^{-\beta E_{i-1}}\right)\right]$

Where N_ℓ = Number of Events in Energy Loss Interval ℓ Which Has Upper Bound E_ℓ Lower Bound $E_{\ell-1}$.

FIG. 9. General equation describing the number of events in a given energy deposition interval due to events in a specified LET interval.

$$\text{Events in LET Interval } j = \sum_{i=1}^{i=j} M_{ij}$$

$$\text{Dose in LET Interval } j = \frac{p}{m}\sum_{i=1}^{i=j} \bar{E}_i M_{ij}$$

$$\text{Dose Equiv. in LET Interval } j = g(j)\,\frac{p}{m}\sum_{i=1}^{i=j} \bar{E}_i M_{ij}$$

where p = constant = 1.60×10^{-9} ERGS/KEV

m = weight of gas in cavity (GM)

$\bar{E}_i$ = average energy of energy loss interval i (KEV)

$g(j)$ = quality factor associated with LET interval j.

FIG. 10. General equations used in calculating the event, dose, and dose equivalent distribution in LET.

and different distribution due to events originating in the cavity gas, is to be expected.[8]

With this uncertainty in mind, the computer program was set up to make the determination using square, triangular, or exponential distribution assumptions, and we routinely calculate all data with both square and triangular assumptions. Techniques for including the noncrossing events are being studied for inclusion in the program.

The computational technique differs somewhat from that of Rossi and Rosenzweig and is similar to spectrum stripping. For an example, let us select the square distribution assumption and no electronic compression. If, in the highest energy loss channel i there are N_i events recorded, then according to the assumptions there are equal numbers of events in each of the lower channels due to particles traversing the chamber on shorter gas paths and having the same LET. Hence, the total number of events of this LET is equal to iN_i. The number N_i is stripped out of each of the i channels, and the process is repeated for the next lower channel. The general equations describing the number of events in a given energy deposition interval due to the events in a given LET interval and the equations for calculating the event, dose, and dose equivalent spectrum are shown in Figs. 9 and 10.

The printout for this step is as follows. The first column is the LET interval, and has direct correspondence to the energy loss interval

in the original data. The second, third, and fourth columns are the number of events, deposited dose, and dose equivalent for the LET interval and the time normalization programmed. The fifth, sixth, and seventh columns are cumulative totals for the same quantities, and the significant cumulative quantities appear in the highest LET interval, being the totals for the run.

6. A third subroutine, primarily for plotting purposes, can be applied selectively to the event, dose, or dose equivalent rate distributions for each of the stripping assumptions programmed. The functions of this subroutine are to determine the average LET for each interval, to normalize the data to unit LET interval, to further smooth from the data some of the irregularities resulting from the stripping program, and to provide various scale information needed by the automatic plotting equipment. A hand-drawn plot of typical output data is in Fig. 11. The case shown is for a 50 channel plutonium–beryllium source spectrum taken with analog computer power funtion of 0.5.

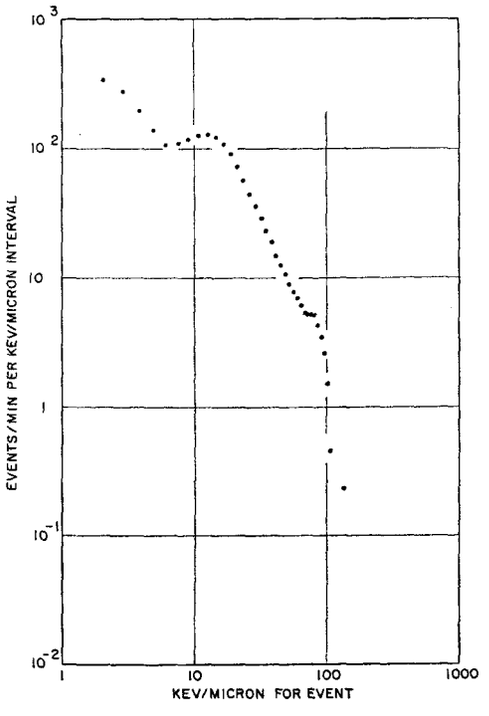

FIG. 11. Plot of output data from computer program. This is the event distribution in LET for a 50 channel spectrum due to Pu-Be neutrons. A total of 130,529 events were analyzed using a square root spectrum compression and assuming a square path length distribution. The typical distribution of data points and degree of smoothing is shown.

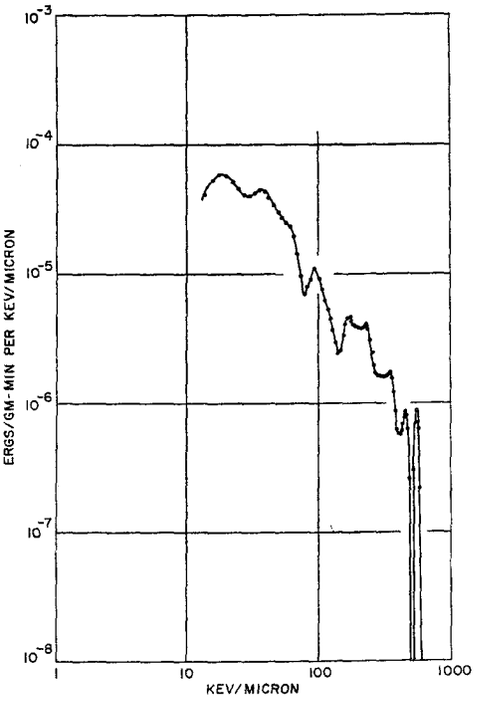

FIG. 12. Dose distribution in LET for plutonium–beryllium neutrons. A total of 107,373 events in 100 channels was analyzed using square root compression, and assuming a square distribution of path lengths.

EXAMPLES OF RESULTS

The following examples of results produced by our system are offered. In each case, the 8-in. diameter chamber was used, the effective cavity diameter was 2.1 microns, and the anode voltage was 660 V.

1. The dose distribution in LET for a plutonium–beryllium source is shown in Fig. 12. The exposure is 80 min at 50 cm from a 4×10^6 n/sec source. The total dose is 2.91 mrad as measured with a tissue equivalent ion chamber of the same dimensions, and a total of 107,373

events were recorded above a 27.2 keV energy loss discriminator level.

2. The dose distribution in LET shown in Fig. 13 is taken under identical conditions to the previous run except that the exposure time was 4 min, resulting in a total dose of 0.145 mrad and a total of 5207 events. As can be seen, the distributions differ only in detail.

3. The dose distribution in LET for a cobalt-60 gamma source is shown in Fig. 14. The exposure is 5.51 mrad for the 40 min run as measured by the ion chamber, resulting in 507,229 events above the 2.0 keV discriminator level. Analysis of the results yields an effective quality factor of 1.09 for this radiation. Since the secondary electrons causing these events do not generally travel in straight line paths across the chamber, the results shown here certainly cannot be accepted at face value.

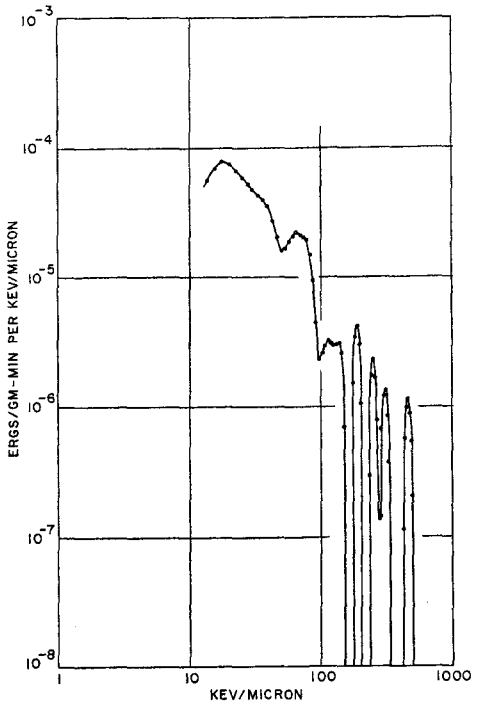

FIG. 13. Dose distribution in LET for plutonium–beryllium neutrons. A total of 5,207 events in 100 channels were analyzed using square root compression and assuming a square distribution of path lengths.

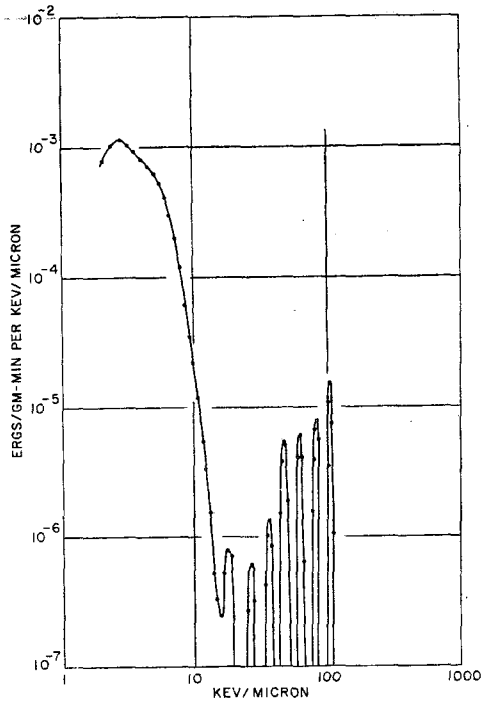

FIG. 14. Dose distribution in LET for cobalt-60 gamma rays. A total of 507,229 events were analyzed using square root compression and assuming a square distribution of path lengths.

4. The dose distribution in LET for a measurement at the Argonne Zero Gradient Synchrotron is shown in Fig. 15. The radiation source was 12.7 BeV protons on a 0.5-in. thick copper target. The detector was placed at a scatter angle of 60° and the shielding at this angle was 5.2 ft of concrete. The detector was located on top of the external proton beam shield. The total dose was 2.25 mrad, measured as before, and resulted in 153,677 events in the 12 min exposure period above a 22.1 keV discriminator level. Analysis of the data indicates an approximate value of 3 for the quality factor.

CONCLUSIONS

An electronic system and computer program has been described which, when utilized with the Rossi LET chamber, produces an assessment of dose, dose equivalent, and quality factor for a radiation field. In addition, distributions in

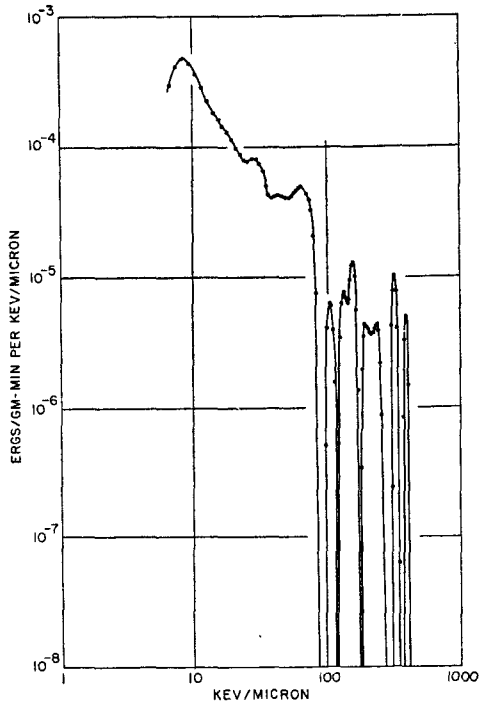

FIG. 15. Dose distribution in LET for radiation from Argonne Zero Gradient Synchrotron. A total of 153,677 events were analyzed using square root compression and assuming a square distribution of path lengths.

LET of the events, dose, and dose equivalent are generated for reasonably small values of dose and consequently short exposure times.

While the system must still be operated by well-trained personnel and the amount of equipment needed to make the measurements is quite impressive, I feel that this system represents a considerable advance in convenience over the currently used systems, and that it attains such improvement without loss in accuracy.

ACKNOWLEDGEMENTS

I would like to express my deepest appreciation to H. R. Sebastian who has assisted in the equipment fabrication, testing, data collection, and preparation of this report. I would also like to thank A. J. Strecok for his assistance in the development of the computer program, and R. W. Fergus for his assistance in design and development in many parts of the electronic circuitry.

REFERENCES

1. H. H. ROSSI and R. ROSENZWEIG. A device for the measurement of dose as a function of specific ionization, *Radiology* **64,** No. 3, 404–410 (March 1955).
2. F. R. SHONKA, J. E. ROSE and G. FAILLA. Conducting plastic equivalent to tissue, air, and polystyrene, *Proc. Second International Conference on Peaceful Uses of Atomic Energy*, Paper 753, Geneva, 1958.
3. Physical aspects of irradiation, *ICRU Handbook* 85, pp. 29–30. National Bureau of Standards, March 1964.
4. Annual Report on Research Project, *NYO*-10050, p. 55. January 1, 1962.
5. H. H. ROSSI and G. FAILLA. Tissue equivalent ionization chambers, *Nucleonics* **14,** No. 2, 32–37 (February 1956).
6. J. KASTNER, J. E. ROSE and F. R. SHONKA. Muscle equivalent environmental radiation meter of extreme sensitivity, *Science* **140,** 1100–1101 (June 7, 1963).
7. M. G. STRAUSS and R. BRENNER. General purpose analog pulse height computer, *Review of Scientific Instruments* **36,** 1857–1876 (December 1965).
8. R. S. CASWELL. Deposition of energy by neutrons in spherical cavities, *Radiation Research* **27,** 92–107 (January 1966).